Femtosecond laser induced surface nanostructures on copper

S.Y. Wang[1], C.W. Cheng[1*], W.C. Shen[1], Y. Ren[2], J.K. Chen[2], D.Y. Tzou[2], and Y. Zhang[2]

[1] *ITRI South, Industrial Technology Research Institute, No. 8, Gongyan Rd., Liujia District, Tainan City 734, Taiwan*

[2] *Department of Mechanical and Aerospace Engineering, University of Missouri, Columbia, Missouri 65211, U.S.A.*

E-mail: CWCheng@itri.org.tw (C.W. Cheng)

This study demonstrated circular surface nanostructures and femtosecond laser-induced periodic surface structures (FLIPSS) for copper produced by a Ti:Sapphire femtosecond laser beam of wavelength 800 nm and duration 120 fs. The circular textured nanostrucres could be created by a single laser pulse. The nanostructures in the center of the heated spot diminish as laser fluence increases and a crater is eventually made at higher fluences. The FLIPSS could only be generated by multiple laser pulses. The resulting periodic ripple-like nanostructures are in a line pattern, and their orientations are perpendicular to the polarization direction. A set of thermal models were also proposed to simulate thermal ablation for copper films, including a two-temperature model, phase change models for melting and evaporation, and phase explosion model. The predicted ablation depths are in good agreement with the existing experimental data.

Keywords: femtosecond laser, nanostructure, two-temperature model

1. Introduction

Functional structures have played a critical role in applications of photovoltaics, light-emitting diodes, biomedicine, and other optical devices. Micro/nano structures, which are one of the major features of functional structures, can be fabricated using methods such as photolithography, electro-beam lithography, focused ion beam lithography, and LIGA (Lithographie, Galvanoformung, Abformung) process, etc. However, these fabrication processes are complicated, high cost, and time consuming.

Femtosecond laser material processing has been demonstrated as a very effective means for micro/nano surface modification of solid materials due to less debris contamination, reproducibility and minimal heat affected zone. When irradiating a metal surface with femtosecond laser pulses, ripples, quasi-periodic nanostructures, or self-organized structures can be directly formed in a simple, one-step process [1, 2]. This technique is referred to as femtosecond laser-induced periodic surface structures (FLIPSS). The term "ripples" or "self-organized structures" refers to the fact that their surface features are formed spontaneously by laser irradiation, with a feature size much smaller than the heated spot size. Examples of the FLIPSS application include preparation of ultra-low reflectance metal surfaces [3-6], surface coloring of stainless steel [7], and surface wettability tuning of various metallics [8-10]. Moreover, the FLIPSS-treated titanium materials have shown potential for implant technology [11] and bacterial retention surface technology [12].

This study demonstrated the circular surface nanostructures and FLIPSS for copper produced by a Ti:Sapphire femtosecond laser beam of wavelength 800 nm and duration 120 fs. The circular textured nanostrucres could be created by a single laser pulse, while multiple laser pulses had to be applied to form the FLIPSS. A numerical simulation was also performed for ultrafast thermal ablation of copper films. The experimental and theoretical results are presented and discussed in the following.

2. Experimental

A commercial copper foil (GTJ-MP, FCFT) of thickness 35 μm was structured in air by an 800-nm wavelength regenerative amplified mode-locked Ti:Sapphire laser (SPITFIRE, Spectra-Physics) operated at a 1 kHz repetition rate. The pulse duration was ~120 fs and the maximum available pulse energy was ~3.5 mJ. The laser beam was linearly polarized and spatially filtered, resulting in an essentially Gaussian profile. The energy of the laser beam was attenuated by a rotatable half-waveplate and a polarizing beam splitter. The transmitted component of the laser beam was incident onto a beam splitter, the reflected beam was directed to a power detector, and the laser irradiation energy on the copper target was measured. Meanwhile, the transmitted linearly-polarized laser beam was passed through a shutter and a series of reflective mirrors, subsequently entering an objective lens (numerical aperture 0.26, M Plan Apo NIR, Mitutoyo). The position of the objective lens was adjusted in the vertical direction (i.e. z-axis), and the focused spot diameter was about 5 μm. Microstructures were produced by translating the target sample using an X–Y stage, and the fabrication process was continuously monitored via a co-axis charge-coupled device (CCD) camera system. The approximately ablation threshold fluence of copper was determined by an optical microscopy. The surface characteristics of the copper were measured using a scanning electron microscopy (SEM, Hitachi S-4700).

The surface structuring on the copper foils was also performed using a single laser pulse. Two kinds of method

were adopted to ensure the single laser pulse effects: (1) single shot trigger and (2) continuous pulse irradiation with a proper scanning speed. For the latter, the laser repetition rate of 1 kHz with a 10 mm/s scanning speed was chosen in this study. The adjacent single shot laser spots were successfully separated.

3. Modeling and Simulation

When the fluence of a femtosecond laser pulse exceeds the ablation threshold, a solid material can be ablated thermally or non-thermally. The former results from ultrafast phase changes through melting, superheating, and vaporization as well as phase explosion, while the latter could be caused by thermal stresses, coulomb explosion, and/or hot electron blast. To accurately simulate the ultrafast thermal ablation process, a set of predictive models are needed, including a two-step heating model for electron temperature (T_e) and lattice temperature (T_l) [13, 14], phase change models [15] for melting and evaporation under superheating, hydrodynamic model for liquid [16] and vapor motion, and phase explosion model for ejection of metastable liquid and bubbles [17, 18]. The details of those predictive models can be found in the above example references and are not discussed here for brevity.

Besides the thermal models themselves, thermophysical and optical properties of materials are another key factors that determine if the theoretical solutions of ultrafast laser material interactions are reliable and accurate or not. Though the thermophysical properties govern thermal transport and temperature distributions, the optical properties are more crucial because they dictate laser energy deposition that can significantly alter the thermal response. To date, the thermophysical properties that have been using in simulations of ultrafast laser heating are quite satisfactory, compared to the optical properties. Through trial and error, either a constant surface reflectivity (R) [18] or the absorbed laser fluence [19], together with a constant absorption coefficient (α) at room temperature, is often chosen in order to match experimental data of ultrafast, ultraintense laser material ablation. Nonetheless, a different value of R or absorbed laser fluence must be selected again when laser heating conditions are changed. The inadequacy is that those approaches are semi-empirical, and the actual values of R and α are never divulged. This, therefore, creates a need for establishing a unique set of temperature-dependent R and α so that the volumetric laser heat source (S) can be correctly described:

$$S(x,t)=0.94\frac{[1-R(0,t)]J_o}{t_p}\alpha(x,t)\exp[-\int_0^x\alpha(x,t)dx-2.77(\frac{t}{t_p})^2] \quad (1)$$

where J_o is laser fluence, t_p is pulse duration, x is spatial coordinate in the laser beam direction with $x = 0$ denoting the irradiated surface, and t is time.

Recently, Ren et al. [20] showed that the critical point model [21] with three Lorentzian terms can accurately characterize surface reflectivity and absorption coefficient of copper for a wide range of laser wavelengths 200-1000 nm. The dielectric permittivity is written in the form:

$$\varepsilon(\omega)=\varepsilon_\infty-\frac{\omega_D^2}{\omega^2+i\gamma\omega}+\sum_{p=1}^{n}B_p\Omega_p\left(\frac{e^{i\phi_p}}{\Omega_p-\omega-i\Gamma_p}+\frac{e^{-i\phi_p}}{\Omega_p+\omega+i\Gamma_p}\right) \quad (2)$$
$$=\varepsilon_1(x,t)+i\varepsilon_2(x,t)$$

where ε_∞ is dielectric constant, ω_D plasma frequency, ω laser frequency, γ damping coefficient which equals reciprocal of electron relaxation time, n a positive integer, B a weighting factor, and Ω, ϕ and Γ energy of gap, phase and broadening, respectively.

The optical properties R and α can be obtained from Fresnel function [22]:

$$R(x,t)=\frac{(f_1(x,t)-1)^2+f_2^2(x,t)}{(f_1(x,t)+1)^2+f_2^2(x,t)} \quad (3)$$

$$\alpha(x,t)=\frac{2\omega f_2(x,t)}{c} \quad (4)$$

where c is light speed in vacuum, and the normal refractive index f_1 and extinction coefficient f_2 are functions of ε_1 and ε_2:

$$f_1(x,t)=\sqrt{\frac{\varepsilon_1+\sqrt{\varepsilon_1^2+\varepsilon_2^2}}{2}} \quad (5)$$

$$f_2(x,t)=\sqrt{\frac{-\varepsilon_1+\sqrt{\varepsilon_1^2+\varepsilon_2^2}}{2}} \quad (6)$$

The electron relaxation time (τ_e) which equals the reciprocal of damping coefficient γ in Eq. (2) can be expressed by:

$$\tau_e=\frac{1}{3.54\upsilon_{e,p}+A_eT_e^2} \quad (7)$$

with [23]

$$\upsilon_{e,ph}=\frac{\Xi^2}{8\pi\varepsilon_F k_F\rho s}\frac{m_{opt}}{m_e}\{\int_0^{q_b}\frac{e^{\phi_l}+e^{\phi_e}}{(e^{\phi_l}-1)(e^{\phi_e}+1)}q^4dq$$
$$+\eta\int_0^{q_b}\frac{e^{\phi_l}-e^{\phi_e}}{(e^{\phi_l}-1)(e^{\phi_e}+1)}q^3dq \quad (8)$$
$$+q_b\frac{e^{\varphi_l}+e^{\varphi_e}}{(e^{\varphi_l}-1)(e^{\varphi_e}+1)}\times\frac{(2k_F)^4-q_b^4}{4}$$
$$-4\eta q_b^2k_F^2\frac{e^{\varphi_l}-e^{\varphi_e}}{(e^{\varphi_l}-1)(e^{\varphi_e}+1)}\}$$

where $\phi_l=\beta_l\hbar qs$ with Planck's constant $h=2\pi\hbar$, $\phi_e=\beta_e\hbar qs$, $\varphi_l=\beta_l\hbar q_b s$, $\varphi_e=\beta_e\hbar q_b s$, ε_F is Fermi energy, k_F Fermi velocity, ρ mass density, s longitudinal sound velocity, m_{opt} effective electron mass, m_e mass of an electron, q phonon wave vector, $\beta_l = T_l/k_B$ with k_B being Boltzmann's constant, $\beta_e = T_e/k_B$, and $\eta=2m_{opt}s/\hbar$. For copper, Ξ = 3.99 eV, $q_b = 8.97\times10^9$ m^{-1}, and $m_{opt} = 1.39\ m_e$. The value of 3.54 in Eq. (7) is set for $\tau_e = 10$ fs at room temperature.

4. Results and Discussion

The SEM images of copper nanostructures fabricated by a single femtosecond laser pulse are shown in Fig. 1 for different fluences of 0.5, 1.0, 1.6, 6.5, 68.9, and 189.6 J/cm^2, respectively. As can be seen in Fig. 1 (a)-(d), the resulting circular textured nanostructures are composed of many nano-bumps and nano-cavities. Apparently, the sizes of the nanocavities reduce as the laser pulse energy decreases. Fig. 2 presents the tilt view SEM image of the case in Fig. 1(c). It can be observed that the nanostructure consists of many cross-linked cavities whose sizes are larger in the center than in the periphery. The nanostructures in the center part diminish as the fluence increases and a crater is

eventually made at higher fluences, for example, 68.9 J/cm^2 and 189.6 J/cm^2. Figure 3 shows the profile of the crater in Fig. 1(f). The transition of change of nanostructures in the center portion can be attributed to the Gaussian profile and intensity of the laser beams. Due to the Gaussian beam property, much more energy is absorbed in the central part of the heated spot than in the outer region. Of consequence, the induced temperatures are much higher in the inner area. The resulting hydrodynamic motion from the superheating and recoil pressure could lead to nanostructures and even to craters that are compounded by thermal ablation, see Figs. 1(e)-(f) and 3.

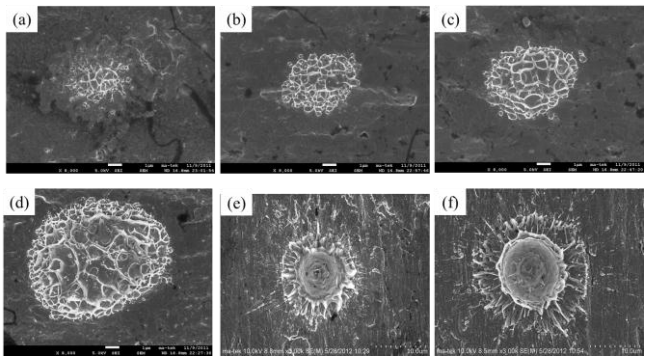

Fig. 1 Top view SEM images of nanostructures of copper generated by a single femtosecond laser pulse at fluences: (a) 0.5 J/cm^2, (b) 1.0 J/cm^2, (c) 1.6 J/cm^2, (d) 6.5 J/cm^2, (e) 68.9 J/cm^2, and (f) 189.6 J/cm^2.

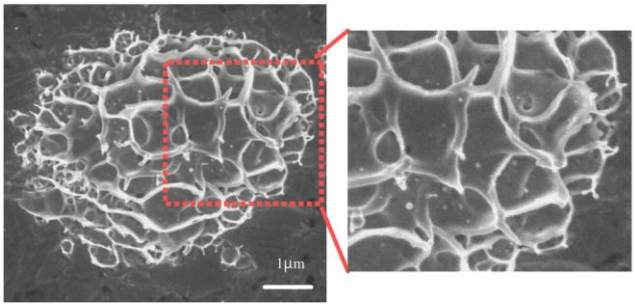

Fig. 2 Tile view SEM image of Fig. 1(c).

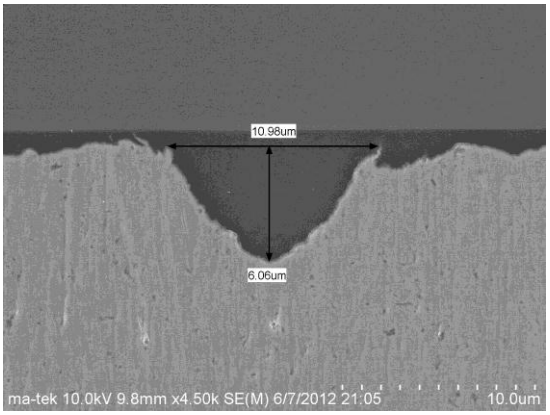

Fig. 3 Profile of the crater of Fig. 1(f).

Fig. 4 presents SEM image of the line pattern of FLIPSS formed by multiple femtosecond laser pulses at fluence 3.2 J/cm^2 and a scanning speed 0.2 mm/s with linearly polarized light orientated in the direction perpendicular to the scanning direction path. These FLIPSS can be made only by multiple laser pulses, as pointed out by Wang and Guo [24]. From the magnification image, a ripple-like characteristic of the line patterns is observed and the orientations of the periodic nanogratings are perpendicular to the polarization direction.

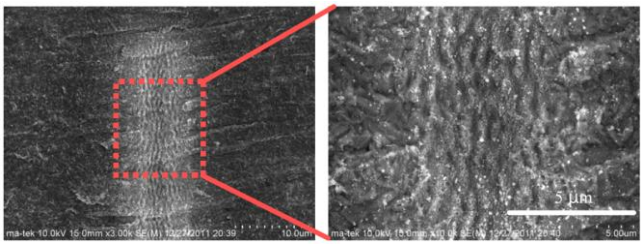

Fig. 4 SEM image of line pattern ripples formed at laser fluence 3.2 J/cm^2 and a scanning speed of 0.2 mm/s with linearly polarized light orientated in the direction perpendicular to the scanning direction path.

Wang and Guo [25] studied the dynamics of femtosecond laser-induced nanostructures formation on noble metals (e.g. Cu, Ag, and Au), showing that generation of the periodic surface nanostructures directly relates to two competing mechanisms, electron-phonon coupling and hot electron diffusion, following the femtosecond laser irradiation. By imposing an additional periodic spatial distribution to laser energy density, they demonstrated numerically that the surface lattice temperature is highly non-uniform if the strong electron-phonon coupling is strong. This is because more energy is transferred from the hot electrons to the lattice, compared to the energy diffused from the hot electrons to the surrounding cold electrons. Very recently, Colombier et al. [26] further studied the ripples growth on femtosecond laser irradiated metals. They also suggested that electron-phonon coupling strength is the key factor that influences the ripples growth on metals. When the electron-phonon coupling is strong, a thin layer is molten and the ripples growth is expected due to the sharp temperature gradient.

In the theoretical study, a one-dimensional approach is assumed for the two-step laser heating [14] with ultrafast phase changes for melting and evaporation [15] and phase explosion [17,18]. Hydrodynamic motion is not considered at the time being. A total of 2500 finite volumes are modeled in a 1.0 μm copper film. The nonlinear numerical algorithms for simulating the solid-liquid and liquid-vapor phase changes can be found in Ren et al. [15]. When the calculated temperature of liquid lattice reaches 90% of the critical equilibrium temperature (T_c = 7696 K for copper [27]), the superheated liquid is assumed to undergo a homogeneous bubble nucleation at an extremely high rate. As a result of the tremendous amount of bubble nuclei rapidly formed, the material in the near-surface region relaxes explosively into a mixture of vapor and equilibrium liquid droplets and is immediately ejected from the bulk material. In the numerical simulation, the value of A_e in Eq. (7) is 4.0×10^7 K^{-2}s^{-1} and the other thermophysical properties and parameters for the optical properties employed can be found in Reference [20].

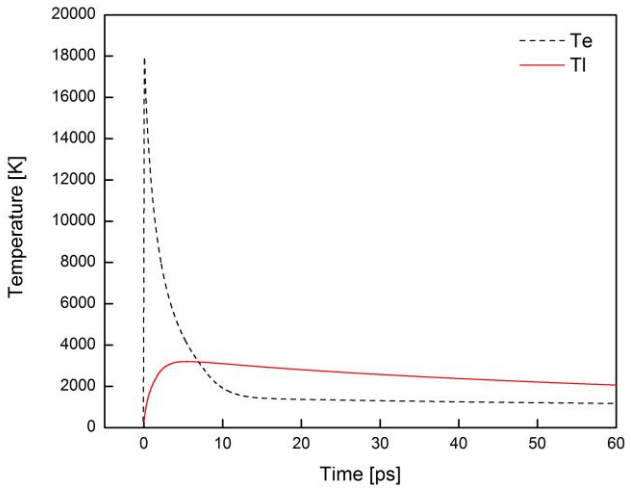

Fig. 5 Time evolution of electron and lattice temperature at the front surface of a 1-μm copper film heated by a femtosecond laser pulse of 70 fs, 800 nm and 0.5 J/cm^2.

Figure 5 shows the time evolution of electron and lattice temperature at the front (x = 0) surface of the copper film irradiated by a single laser pulse of 70 fs, 800 nm and 0.5 J/cm^2. It can be seen that through the strong electron-phonon coupling T_e quickly becomes equal to T_l, at about t = 6.9 ps. The two temperatures, however, do not stay the same afterwards. In fact, T_e keeps on falling at a faster rate than T_l does for several picoseconds. Then, the difference of the two temperatures gradually diminishes until the thermal equilibrium establishes. The non-equilibrium between T_e and T_l in this stage is due to the fact that the diffusion of electron thermal energy predominates over the energy exchange between electrons and the lattice.

The superheating behavior is demonstrated in Fig. 6 by the distributions of lattice temperature in the front part (0-100 nm) of the copper film. It can be clearly seen from the figure that the peak temperature occurs inside the film as early as t = 3 ps, indicating that the superheating process of melting already takes place. The bottom of the valley is the temperature at the solid-liquid interface. On the other hand,

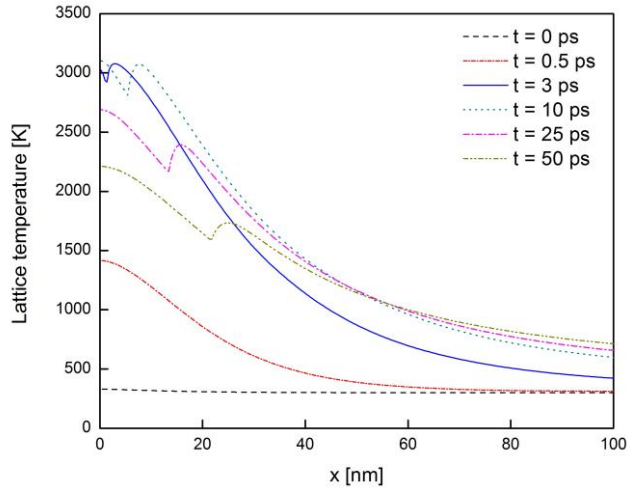

Fig. 6 Lattice temperature distributions in the 0-100 nm depth of the copper film heated by the femtosecond laser pulse of 70 fs, 800 nm and 0.5 J/cm^2.

the lower temperature at the front surface than in the adjacent region means that evaporation also occurs from the front surface though for a much shorter time (2.4-19.1 ps). No phase explosion is simulated at this laser fluence since the temperatures are much smaller than the critical equilibrium temperature.

Figure 7 shows the time history of laser material ablation for three different fluences. It is evident that the greater the fluence is, the earlier the sputtering starts, the later the sputtering completes, and the more the material is ablated.

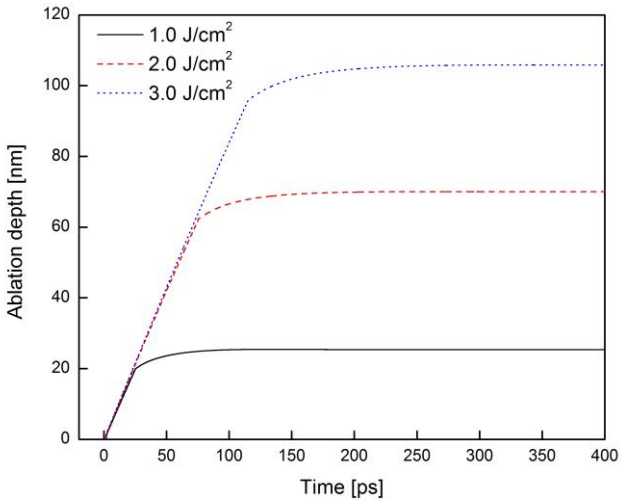

Fig. 7 Ablation depth against time for different laser fluences.

Figure 8 compares the ablation rate between the measurements [28] and the present simulation. Both the experimental data were averaged by dividing the total ablation depth by the total number of laser pulses applied. It appears that the present theoretical results are in good agreement with the experimental data except for lower fluence, where ablation is mainly dominated by the non-thermal mechanism. It should be noted that the simulated amount of material ablated through vaporization is very small compared to that through phase explosion.

4. Conclusions

This study demonstrated the surface nanostructures and FLIPSS for copper produced by a Ti:Sapphire femtosecond laser beam of wavelength 800 nm and duration 120 fs. The circular textured nanostrucres can be created by a single laser pulse. The resulting circular textured nanostructures consist of many nano-bumps and nanocavities, and the sizes of the nanocavities increase with laser pulse energy. The nanostructures in the center of the heated spot diminish as laser fluence increases and a crater is eventually made at higher fluences, for example, 68.9 J/cm^2. The change of nanostructures in the central part can be attributed to much more laser energy deposited in the centers of the heated spots. On the other hand, the FLIPSS can only be created by multiple laser pulses. The resulting periodic ripple-like nanostructures are in a line pattern; their orientations are perpendicular to the polarization direction. It is believed that the electron-phonon coupling

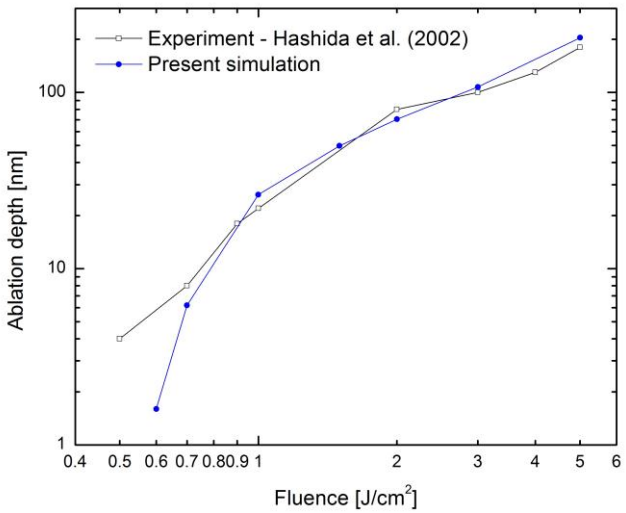

Fig. 8 Comparison of ablation depth between the present simulation and experimental data [28].

strength is one of the key factors that influence the ripples formation. A set of thermal models are also proposed to simulate ultrafast thermal ablation of copper metal, including a two-temperature model, phase change models for melting and evaporation, and phase explosion model. The predicted ablation depths for copper films are in good agreement with the existing experimental data. To simulate the circular textured nanostrucres generated by a single laser pulse and the periodic ripple-like nanostructures made by multiple laser pulses, a comprehensive 3D thermal model with hydrodynamic motion is suggested.

Acknowledgements

The authors would like to thank the Ministry of the Economic Affairs (MOEA), Taiwan, R.O.C. for supporting this project.

References

[1] L. T. Qi, K. Nishii, and Y. Namba, "Regular subwavelength surface structures induced by femtosecond laser pulses on stainless steel," Optics Letters, vol. 34, pp. 1846-1848, 2009.

[2] B. K. Nayak and M. C. Gupta, "Self-organized micro/nano structures in metal surfaces by ultrafast laser irradiation," Optics and Lasers in Engineering, vol. 48, pp. 940-949, 2010.

[3] A. Y. Vorobyev and C. Guo, "Enhanced absorptance of gold following multipulse femtosecond laser ablation," Physical Review B, vol. 72, 195422, 2005.

[4] Y. Yang, J. J. Yang, C. Y. Liang, and H. S. Wang, "Ultra-broadband enhanced absorption of metal surfaces structured by femtosecond laser pulses," Optics Express, vol. 16, pp. 11259-11265, 2008.

[5] B. K. Nayak, M. C. Gupta, and K. W. Kolasinski, "Formation of nano-textured conical microstructures in titanium metal surface by femtosecond laser irradiation," Applied Physics A-Materials Science & Processing, vol. 90, pp. 399-402, 2008.

[6] V. V. Iyengar, B. K. Nayak, and M. C. Gupta, "Ultralow reflectance metal surfaces by ultrafast laser texturing," Applied Optics, vol. 49, pp. 5983-5988, 2010.

[7] B. Dusser, Z. Sagan, H. Soder, N. Faure, J. P. Colombier, M. Jourlin, and E. Audouard, "Controlled nanostructrures formation by ultra fast laser pulses for color marking," Optics Express, vol. 18, pp. 2913-2924, 2010.

[8] M. N. W. Groenendijk and J. Meijer, "Surface microstructures obtained by femtosecond laser pulses," Cirp Annals-Manufacturing Technology, vol. 55, pp. 183-186, 2006.

[9] G. R. B. E. Romer, A. J. Huis in't Veld, J. Meijer, and M. N. W. Groenendijk, "On the formation of laser induced self-organizing nanostructures," Cirp Annals-Manufacturing Technology, vol. 58, pp. 201-204, 2009.

[10] A. M. Kietzig, S. G. Hatzikiriakos, and P. Englezos, "Patterned Superhydrophobic Metallic Surfaces," Langmuir, vol. 25, pp. 4821-4827, 2009.

[11] A. Y. Vorobyev and C. Guo, "Femtosecond laser structuring of titanium implants," Applied Surface Science, vol. 253, pp. 7272-7280, 2007.

[12] E. Fadeeva, V. K. Truong, M. Stiesch, B. N. Chichkov, R. J. Crawford, J. Wang, and E. P. Ivanova, "Bacterial Retention on Superhydrophobic Titanium Surfaces Fabricated by Femtosecond Laser Ablation," Langmuir, vol. 27, pp. 3012-3019, 2011.

[13] S. I. Anisimov, B. L. Kapeliovich, and T. L. Perel'man, "Electron emission from metal surfaces exposed to ultrashort laser pulses," Soviet Physics, Journal of Experimental and Theoretical Physics, vol. 39, pp. 375-377, 1974.

[14] J. K. Chen and J. E. Beraun, "Numerical study of ultrashort laser pulse interactions with metal films," Numerical Heat Transfer Part A, vol. 40, pp. 1-20, 2001.

[15] Y. Ren, J. K. Chen, and Yuwen Zhang, "Modeling of ultrafast phase changes in metal films irradiated by an ultrashort laser pulse using a semiclassical two-temperature model," International Journal Heat and Mass Transfer, vol. 55, pp. 1260-1627, 2012.

[16] J. P. Colombier, P. Combis, F. Bonneau, R. Le Harzic, and E. Audouard, "Hydrodynamic simulations of metal ablation by femtosecond laser irradiation," Physical Review B, vol. 71, 165406, 2005.

[17] R. Kelly and A. Miotello, "Comments on explosive mechanisms of laser sputtering," Applied Surface Science, vol. 96-98, pp. 205-215, 1996.

[18] J. K. Chen, J. E. Beraun, and D. Y. Tzou, "Investigation of ultrafast laser ablation using a semiclassical two-temperature model," Journal of Directed Energy, vol. 1, pp. 261-274, 2005.

[19] J. Byskov-Nielsen, J.-M. Savolainen, M. S. Christensen, and P. Balling, "Ultra-short pulse laser ablation of copper, silver and tungsten: experimental data and two-temperature model simulations," Applied Physics A-Materials Science & Processing, vol. 103, pp. 447-453, 2011.

[20] Y. Ren, J. K. Chen, and Y. Zhang, "Optical properties and thermal response of copper films induced by ultrashort-pulsed lasers," Journal of Applied Physics, vol. 110, 113102, 2011.

[21] P. G. Etchegoin, E. C. Le Ru, and M. Meyer, "An analytic model for the optical properties of gold," Journal of Chemical Physics, vol. 125, 164705, 2006.
[22] M. Fox, Optical Properties of Solids: Oxford University Press, Oxford, 2010.
[23] D. Fisher, M. Frankel, Z. Henis, E. Moshe, and S. Eliezer, "Interband and intraband (Drude) contributions to femtosecond laser absorption in aluminum," Physical Review E, vol. 65, 266107, 2002.
[24] J. C. Wang and C. L. Guo, "Ultrafast dynamics of femtosecond laser-induced periodic surface pattern formation on metals," Applied Physics Letters, vol. 87, 251914, 2005.
[25] J. C. Wang and C. L. Guo, "Numerical study of ultrafast dynamics of femtosecond laser-induced periodic surface structure formation on noble metals," Journal of Applied Physics, vol. 102, 053522, 2007.
[26] J. P. Colombier, F. Garrelie, N. Faure, S. Reynaud, M. Bounhalli, E. Audouard, R. Stoian, and F. Pigeon, "Effects of electron-phonon coupling and electron diffusion on ripples growth on ultrafast-laser-irradiated metals," Journal of Applied Physics, vol. 111, 024902, 2012.
[27] H. Hess, "Critical data and vapor pressures of aluminium and copper," Zeitschrift für Metallkunde, vol. 89, pp. 388-393, 1998.
[28] M. Hashida, A. F. Semerok, O. Gobert, G. Petite, Y. Izawa, and J. F. Wagner, "Ablation threshold dependence on pulse duration for copper," Applied Surface Science, vol. 197, pp. 862-867, 2002.